Nuclear Physics A519 (1990) 548–566
North-Holland

SIGNATURE-DEPENDENT EFFECTS OF GAMMA VIBRATION ON E2 TRANSITIONS IN ROTATING ODD-*A* NUCLEI

(II). Triaxial nuclei

Masayuki MATSUZAKI

Institute of Physics, University of Tsukuba, Ibaraki 305, Japan

Received 17 April 1990
(Revised 23 July 1990)

Abstract: Signature-dependent effects of gamma vibration on properties of rotating odd-*A* nuclei are studied by means of the quasiparticle–vibration-coupling approach based on the cranking-plus-RPA formalism. In the first half of this paper, the signature dependence and the shell-filling dependence of both the quasiparticle–vibration-coupling wave function and of the E2 transitions in the $\gamma = 0$ case are discussed. The gamma-vibrational effect on $B(\mathrm{E2}: I \to I-2)$ is shown to be weaker than that on $B(\mathrm{E2}: I \to I-1)$. In the second half, the vibrational effect on $B(\mathrm{E2}: I \to I-1)$ in $\gamma \neq 0$ cases is shown to defeat the effect of the static gamma deformation of the rotating potential when $\gamma^{(\mathrm{pot})}$ is smaller than the zero-point amplitude γ_0. A prediction is given for the signature and the shell-filling dependence of $B(\mathrm{E2}: I \to I-1)$ and for the sign change of E2/M1 mixing ratio in an experimentally accessible isotope chain, $^{159\text{-}169}$Yb.

1. Introduction

Excited quasiparticles as well as collective rotation can induce the shape change of nuclei. The shape polarization effect of quasiparticles on rotating cores is becoming recognized in terms of the shell correction method. In order to study the gamma degree of freedom in rotating nuclei further, its dynamical aspect should be considered. It has been discussed mainly in the context of the signature dependence of level energies and $B(\mathrm{M1}: I \to I-1)$ values, about which rich experimental information is available. In contrast, data of $B(\mathrm{E2}: I \to I-1)$ values are limited although they are expected to carry more direct knowledge of triaxiality. The first observation of strong signature dependence of $B(\mathrm{E2}: I \to I-1)$ was reported by Hagemann *et al.* [1]. Although this datum was revised later [2], it stimulated the theoretical studies about the effects of static and dynamic triaxialities [3–10].

Among them, we discussed the phase rule of the signature dependence of $B(\mathrm{E2}: I \to I-1)$ due to the static triaxial deformation of the rotating potential, and presented some numerical examples on the basis of the cranking picture in refs. [7,8]. In ref. [9]), to which we will refer henceforth as paper (I), we clarified the phase rule of the signature dependence due to the gamma vibration around an axially symmetric shape and its shell-filling dependence, both analytically and numerically. This work was motivated by the result in ref. [7]) that the effect of gamma vibration is stronger than that of the static gamma deformation of rotating potential.

The purpose of the present paper is to extend the study on the vibrational effect on $B(\mathrm{E2}: I \to I-1)$ in the $\gamma = 0$ case developed in paper (I) to two directions: firstly, to other quantities mainly in the $\gamma = 0$ case, and secondly, to $B(\mathrm{E2}: I \to I-1)$ in axially asymmetric cases.

This paper consists of two parts. The first part includes sects. 2 and 3. In sect. 2, detailed properties of quasiparticle-vibration-coupling wave functions are discussed. The coupling schemes in various models are also mentioned. In sect. 3, the gamma-vibrational effect on $B(\mathrm{E2}: I \to I-2)$ in axially symmetric nuclei is discussed comparing with that on $B(\mathrm{E2}: I \to I-1)$. Sects. 4 and 5 correspond to the second part. Sect. 4 is the core of the present paper. Here the competition of the static and dynamic deformations is investigated by evaluating the signature dependence of $B(\mathrm{E2}: I \to I-1)$ values. The meaning of γ in the present approach is also discussed in this section. The competition mentioned above and the sign change of E2/M1 mixing ratio due to the coupling with gamma vibration in an experimentally accessible isotope chain are studied in sect. 5. Sect. 6 is devoted to concluding remarks.

2. Properties of quasiparticle–vibration-coupling wave functions

The quasiparticle-vibration-coupling hamiltonian in the cranking-plus-RPA formalism can be derived from the pairing plus doubly-stretched quadrupole interaction in rotating frame, and takes the form:*

$$\begin{aligned} H_{\mathrm{coupl}}(\gamma) = & \sum_{\mu\nu}{}'' \Lambda_{\gamma}^{(+)}(\mu\nu)(X_{\gamma(+)}^{\dagger} a_{\mu}^{\dagger} a_{\nu} + X_{\gamma(+)} a_{\nu}^{\dagger} a_{\mu}) \\ & + \sum_{\mu\bar{\nu}} \Lambda_{\gamma}^{(-)}(\mu\bar{\nu})(X_{\gamma(-)}^{\dagger} a_{\mu}^{\dagger} a_{\bar{\nu}} + X_{\gamma(-)} a_{\bar{\nu}}^{\dagger} a_{\mu}) \\ & + \sum_{\mu\bar{\nu}} \Lambda_{\gamma}^{(-)}(\bar{\nu}\mu)(X_{\gamma(-)}^{\dagger} a_{\bar{\nu}}^{\dagger} a_{\mu} + X_{\gamma(-)} a_{\mu}^{\dagger} a_{\bar{\nu}}) . \end{aligned} \tag{2.1}$$

Here $a_{\mu}^{\dagger}$ and $a_{\bar{\mu}}^{\dagger}$ denote quasiparticles with the signature quantum number $r = -i$ and $+i$, respectively, while $X_{\gamma(\pm)}^{\dagger}$ denotes gamma-vibrational phonons with $r = \pm 1$. The coupling vertices are also classified by $r = \pm 1$, and are given by**

$$\begin{aligned} \Lambda_{\gamma}^{(+)}(\mu\nu) &= -\sum_{K=0,1,2} \kappa_K^{(+)} \tilde{T}_K^{(+)} \tilde{Q}_K^{(+)}(\mu\nu) , \\ \Lambda_{\gamma}^{(-)}(\mu\bar{\nu}) &= -\sum_{K=1,2} \kappa_K^{(-)} \tilde{T}_K^{(-)} \tilde{Q}_K^{(-)}(\mu\bar{\nu}) , \\ \Lambda_{\gamma}^{(-)}(\bar{\nu}\mu) &= -\sum_{K=1,2} \kappa_K^{(-)} \tilde{T}_K^{(-)} \tilde{Q}_K^{(-)}(\bar{\nu}\mu) , \end{aligned} \tag{2.2}$$

where the force strengths $\kappa_K^{(\pm)}$ are positive and the transition amplitudes are defined as

$$\tilde{T}_K^{(\pm)} = [\tilde{Q}_K^{(\pm)}, X_{\gamma(\pm)}^{\dagger}]_{\mathrm{RPA}} , \tag{2.3}$$

with $\tilde{Q}_K^{(\pm)}$'s denoting the doubly-stretched quadrupole operators [11]).

* The double prime attached to $\sum$ denotes that when the component $(\mu\nu)$ is summed its signature partner $(\bar{\mu}\bar{\nu})$ should also be summed.

** The contributions from the residual pairing interaction in the $r = +1$ sector are omitted in this expression for simplicity.

When the single-j approximation holds well and $j+\frac{1}{2}=$ even (odd), usually the states with $r=+i$ $(-i)$ lie lower in energy than their signature partners and are called the favored (f) states. Their partners are called the unfavored (u) states. As shown in paper (I), the vertices $\Lambda_\gamma^{(-)}$ can be rewritten in terms of $|\mathrm{f}\rangle$ and $|\mathrm{u}\rangle$ utilizing the symmetry property [11])

$$\tilde{Q}_K^{(-)}(\mu\bar{\nu}) = -(-1)^K \tilde{Q}_K^{(-)}(\bar{\nu}\mu)\,. \tag{2.4}$$

For those concerning the lowest-energy quasiparticle state with each signature, we adopt the notation:

$$\begin{aligned}
\Lambda_\gamma^{(-)}(\gamma\mathrm{f},\mathrm{u}) &= -(\kappa_1^{(-)}\tilde{T}_1^{(-)}\langle \mathrm{f}|\tilde{Q}_1^{(-)}|\mathrm{u}\rangle + \kappa_2^{(-)}\tilde{T}_2^{(-)}\langle \mathrm{f}|\tilde{Q}_2^{(-)}|\mathrm{u}\rangle)\,,\\
\Lambda_\gamma^{(-)}(\gamma\mathrm{u},\mathrm{f}) &= -(\kappa_1^{(-)}\tilde{T}_1^{(-)}\langle \mathrm{f}|\tilde{Q}_1^{(-)}|\mathrm{u}\rangle - \kappa_2^{(-)}\tilde{T}_2^{(-)}\langle \mathrm{f}|\tilde{Q}_2^{(-)}|\mathrm{u}\rangle)\,.
\end{aligned} \tag{2.5}$$

The former denotes the coupling strength between $|\mathrm{u}\rangle$ and $X^\dagger_{\gamma(-)}|\mathrm{f}\rangle$ while the latter denotes the one between $|\mathrm{f}\rangle$ and $X^\dagger_{\gamma(-)}|\mathrm{u}\rangle$. The vertices $\Lambda_\gamma^{(+)}$ concerning the lowest-energy states are given by

$$\begin{aligned}
\Lambda_\gamma^{(+)}(\gamma\mathrm{f},\mathrm{f}) &= -\sum_{K=0,2}\kappa_K^{(+)}\tilde{T}_K^{(+)}\langle \mathrm{f}|\tilde{Q}_K^{(+)}|\mathrm{f}\rangle\,,\\
\Lambda_\gamma^{(+)}(\gamma\mathrm{u},\mathrm{u}) &= -\sum_{K=0,2}\kappa_K^{(+)}\tilde{T}_K^{(+)}\langle \mathrm{u}|\tilde{Q}_K^{(+)}|\mathrm{u}\rangle\,.
\end{aligned} \tag{2.6}$$

Here we note that the diagonal matrix elements of $\tilde{Q}_1^{(+)}$ vanish due to the antihermiticity. The $K=1$ term in eq. (2.5) and the $K=0$ term in eq. (2.6) originate from the Coriolis perturbation to gamma vibrations in the first and second order, respectively. Therefore, we can expect that $|\tilde{T}_1^{(-)}/\tilde{T}_2^{(-)}| \gg |\tilde{T}_0^{(+)}/\tilde{T}_2^{(+)}|$. For example, the left-hand side is 0.33–0.40 while the right-hand side is 0.06–0.12 in the numerical calculation presented later.

Gamma vibrations with $r=+1$ and -1, which we call the $\gamma(+)$ and $\gamma(-)$ vibrations henceforth, contribute to $B(\mathrm{E2})$'s with $\Delta I=2$ and 1, respectively, in the first order (see sect. 3). Referring to this fact, we concentrate our attention on the first-order perturbation wave functions with respect to the quasiparticle-vibration-coupling hamiltonian (2.1) in the following. They are given by

$$\begin{aligned}
|\mathrm{u}\rangle\!\rangle &= a_\mathrm{u}^\dagger|\phi\rangle + \delta_\mathrm{u}^{(-)}a_\mathrm{f}^\dagger X^\dagger_{\gamma(-)}|\phi\rangle + \delta_\mathrm{u}^{(+)}a_\mathrm{u}^\dagger X^\dagger_{\gamma(+)}|\phi\rangle\,,\\
|\mathrm{f}\rangle\!\rangle &= a_\mathrm{f}^\dagger|\phi\rangle + \delta_\mathrm{f}^{(-)}a_\mathrm{u}^\dagger X^\dagger_{\gamma(-)}|\phi\rangle + \delta_\mathrm{f}^{(+)}a_\mathrm{f}^\dagger X^\dagger_{\gamma(+)}|\phi\rangle\,,
\end{aligned} \tag{2.7}$$

with

$$\begin{aligned}
\delta_\mathrm{u}^{(-)} &= \frac{\Lambda_\gamma^{(-)}(\gamma\mathrm{f},\mathrm{u})}{\Delta E - \hbar\omega_{\gamma(-)}}, \qquad \delta_\mathrm{u}^{(+)} = \frac{\Lambda_\gamma^{(+)}(\gamma\mathrm{u},\mathrm{u})}{-\hbar\omega_{\gamma(+)}},\\
\delta_\mathrm{f}^{(-)} &= \frac{\Lambda_\gamma^{(-)}(\gamma\mathrm{u},\mathrm{f})}{-\Delta E - \hbar\omega_{\gamma(-)}}, \qquad \delta_\mathrm{f}^{(+)} = \frac{\Lambda_\gamma^{(+)}(\gamma\mathrm{f},\mathrm{f})}{-\hbar\omega_{\gamma(+)}}.
\end{aligned} \tag{2.8}$$

Here $|\phi\rangle$ denotes the yrast configuration of the even-even core and $\Delta E = E_u - E_f$ is the signature splitting of quasiparticle routhian.

The signature dependence of the mixing amplitudes of the $\gamma(-)$ vibrational states, $\delta_u^{(-)}$ and $\delta_f^{(-)}$, is determined by combining the phase rule of $\langle f|\tilde{Q}_K^{(-)}|u\rangle$'s and that of $\tilde{T}_K^{(-)}$'s. We showed in paper (I) that $\langle f|\tilde{Q}_1^{(-)}|u\rangle$ and $\langle f|\tilde{Q}_2^{(-)}|u\rangle$ have the same sign in most cases under the single-j approximation and under such an assumption that the aligned angular momentum of the odd quasiparticle is a constant. The relative sign between $\tilde{T}_1^{(-)}$ and $\tilde{T}_2^{(-)}$ associated with the lowest-energy collective mode was shown to be a function of gamma deformation [12]). Here we should emphasize that this rule holds when the shape of the potential and that of the density are consistent. This means that $\tilde{T}_1^{(-)}/\tilde{T}_2^{(-)}$ is positive irrespective of input $\gamma^{(\mathrm{pot})}$ values for one-quasiparticle bands since the self-consistent gamma deformation of zero-quasiparticle cores is negative (see sect. 4). As a result, $\tilde{T}_1^{(-)}\langle f|\tilde{Q}_1^{(-)}|u\rangle$ and $\tilde{T}_2^{(-)}\langle f|\tilde{Q}_2^{(-)}|u\rangle$ in both relations of eq. (2.5) have the same sign, and then the $\gamma(-)$ vibration mixes strongly to the unfavored states.

This result corresponds to the tilted coupling scheme pointed out by Hamamoto [13]): in the unfavored states of triaxially-deformed nuclei with spins not so high, the rotation axis deviates from principal axes. This correspondence is brought by the idea that the wobbling motion is the high-spin continuation of the $\gamma(-)$ vibration [14,12]). The result that the $\gamma(-)$ vibration makes $B(\mathrm{E2}:\mathrm{f}\to\mathrm{u})$ larger than $B(\mathrm{E2}:\mathrm{u}\to\mathrm{f})$ in both $\gamma=\pm 15°$ cases [7]) like in a particle-rotor calculation [3]) supports the above correspondence (see sect. 4).

The situation is simpler for the positive-signature amplitudes, $\delta_u^{(+)}$ and $\delta_f^{(+)}$. Since $|\tilde{T}_2^{(+)}| \gg |\tilde{T}_0^{(+)}|$ holds for the $\gamma(+)$ vibrational phonons, the difference between $\delta_u^{(+)}$ and $\delta_f^{(+)}$ is determined primarily by the difference between $\langle u|\tilde{Q}_2^{(+)}|u\rangle$ and $\langle f|\tilde{Q}_2^{(+)}|f\rangle$. A numerical example for ^{159}Tm can be found in table 1 of ref. [8]); in this case the proton Fermi surface lies around $\varepsilon_{7/2}$ and accordingly the $\gamma(+)$ vibrational component is larger in the favored one-quasiparticle states than in the unfavored states (see the following discussion about the shell-filling dependence).

Next we discuss the shell-filling (or chemical potential λ) dependence of signature-dependent properties of the quasiparticle-vibration-coupling wave functions presented above. In the following, we assume that the shell-filling dependence of collective properties is weak. According to the discussion in paper (I), the shell-filling dependence of $\delta_u^{(-)}$ and $\delta_f^{(-)}$ is determined by the relation:

$$\frac{\langle f|Q_1^{(-)}|u\rangle}{\langle f|J_z|u\rangle} = \frac{\hbar\omega_{\mathrm{rot}}}{\sqrt{3}\alpha_0}\left\{\left(\frac{\Delta E}{\hbar\omega_{\mathrm{rot}}}\right)^2 - 1\right\}, \tag{2.9}$$

which holds exactly in axially symmetric nuclei. Here α_0 is a quadrupole deformation parameter of rotating potential:

$$h' = h_{\mathrm{sph}} - \alpha_0 Q_0^{(+)} - \hbar\omega_{\mathrm{rot}} J_x . \tag{2.10}$$

As shown in fig. 1 of paper (I), $\langle f|Q_1^{(-)}|u\rangle$ and $\langle f|Q_2^{(-)}|u\rangle$ (and the corresponding

doubly-stretched quantities at the same time) change their signs* around $\lambda \sim \varepsilon_{3/2}$ according to the λ-dependent change in the magnitude of ΔE in eq. (2.9). The signs of $\delta_u^{(-)}$ and $\delta_f^{(-)}$ change around $\lambda \sim \varepsilon_{3/2}$ consequently. The positive-signature amplitudes $\delta_u^{(+)}$ and $\delta_f^{(+)}$ are also governed by eq. (2.9) through the relation [15]):

$$\langle f|Q_2^{(+)}|f\rangle \simeq -\langle u|Q_2^{(+)}|u\rangle \simeq -\langle f|J_z|u\rangle\langle f|Q_2^{(-)}|u\rangle \tag{2.11}$$

(see fig. 1 of ref. [15])), because $\langle f|Q_2^{(-)}|u\rangle$ shows similar shell-filling dependence to that of $\langle f|Q_1^{(-)}|u\rangle$ (see fig. 1 of paper (I)). We note here that the relation (2.11) plays an important role for discussing the shell-filling dependence of the signature inversion in quasiparticle energy [15]).

A numerical example of the shell-filling dependent behavior of the wave function is shown in fig. 1. Quantities in the $r=+1$ and -1 sectors are placed at the left and right, respectively. These are calculated adopting the same parameter set as that used in figs. 1-3 of paper (I): $\hbar\omega_{rot}=0.2$ MeV, $\beta^{(pot)}=0.2$, $\gamma^{(pot)}=0$, $\Delta_n=\Delta_p=1.0$ MeV and the chemical potentials determined so as to give $N=90$ and each Z (=55-71) at $\hbar\omega_{rot}=0$. The RPA calculation was performed in a model space consisting of $N_{osc}=4$-6 for neutrons and $N_{osc}=3$-5 for protons. The quadrupole and pairing force strengths were chosen so as to reproduce $\hbar\omega_{\gamma(\pm)}=0.8$ MeV, $\hbar\omega_\beta=1.0$ MeV, $\hbar\omega_{NG(\pm)}=0$ and the above $\Delta_n=\Delta_p$ at $\hbar\omega_{rot}=0$. In the top panel, single-quasiparticle matrix elements, diagonal $\langle f|Q_2^{(+)}|f\rangle$ and $\langle u|Q_2^{(+)}|u\rangle$ in the $r=+1$ sector and $\langle f|Q_1^{(-)}|u\rangle$ and $\langle f|Q_2^{(-)}|u\rangle$ between the signature partners in the $r=-1$ sector, are shown. Their shell-filling dependence is determined by eqs. (2.9) and (2.11) as discussed in paper (I) and ref. [15]). The perturbation amplitudes are shown in the middle. Positive-signature amplitudes $\delta_f^{(+)}$ and $\delta_u^{(+)}$ are connected directly to the matrix elements of $Q_2^{(+)}$. In the $r=-1$ sector, $K=1$ and 2 terms contribute constructively to $\delta_u^{(-)}$ and destructively to $\delta_f^{(-)}$. In addition to the terms in eq. (2.7), $H_{coupl}(\gamma)$ (eq. (2.1)) brings other one-phonon ($\gamma(+)$ and $\gamma(-)$) components in the lowest-energy quasiparticle-vibration coupling states. The probabilities of one-$\gamma(+)$ and one-$\gamma(-)$ components in these states with $r=+i$ (f) and $r=-i$ (u) are shown in the bottom panel. This is a result of diagonalization. Fig. 1 illustrates that the behavior of the probabilities is determined predominantly by the main amplitudes in the middle panel.

The sum of the mixing probabilities of the $\gamma(+)$ and $\gamma(-)$ components is larger in the unfavored state in the low-λ region while it is larger in the favored state in the high-λ region. The result for the high-λ cases coincides with that of a particle-rotor-model calculation for ^{157}Ho performed by Ikeda [4]). In the interacting boson-fermion model, the exchange interaction makes both the $\gamma(+)$ and $\gamma(-)$ components

* In actual calculations, the overall signs of matrix elements are indefinite except diagonal ones like $\langle f|Q_2^{(+)}|f\rangle$ (see eq. (2.11)); only the relative signs between them, between $\langle f|Q_1^{(-)}|u\rangle$ and $\langle f|J_z|u\rangle$ for instance, are physical. Since the absolute value of $\langle f|J_z|u\rangle=\langle u|J_z|f\rangle$ indicates the effective K-value, henceforth we regard this matrix element as positive. Then the signs of others are determined uniquely referring to it. The situation is similar for the transition amplitudes $\tilde{T}_K^{(\pm)}$ made up from two-quasiparticle matrix elements; we regard $\tilde{T}_2^{(\pm)}$ as positive.

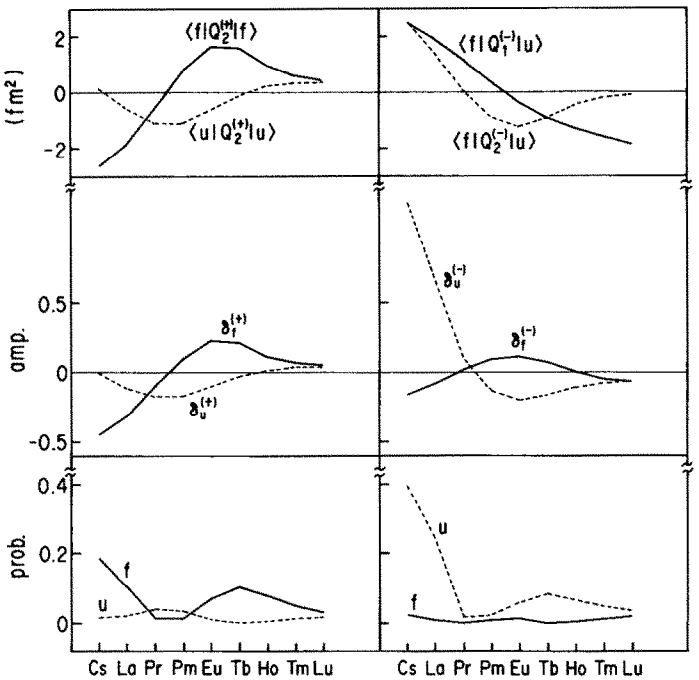

Fig. 1. Single-quasiparticle matrix elements of quadrupole operator (top panel), the first-order mixing amplitudes of the lowest-energy gamma-vibrational components (middle panel), and the total mixing probabilities of one-$\gamma(+)$ and one-$\gamma(-)$ components obtained by diagonalization including up to two-phonon states (bottom panel) calculated at $\hbar\omega_{\rm rot} = 0.2$ MeV and $\gamma^{(\rm pot)} = 0$. Quantities in the $r = +1$ (-1) sector are placed at the left (right). The overall sign of matrix elements was chosen so that $\langle f|J_z|u\rangle$ and $\tilde{T}_2^{(\pm)}$ were positive. Other parameters are $\beta^{(\rm pot)} = 0.2$, $\Delta_n = \Delta_p = 1.0$ MeV, and the chemical potentials determined so as to give $N = 90$ and each Z at $\hbar\omega_{\rm rot} = 0$. The force strengths of the pairing plus doubly-stretched quadrupole interaction were chosen so as to give the above $\Delta_n = \Delta_p$, $\hbar\omega_{\gamma(\pm)} = 0.8$ MeV, $\hbar\omega_\beta = 1.0$ MeV and $\hbar\omega_{\rm NG(\pm)} = 0$ at $\hbar\omega_{\rm rot} = 0$. The top left figure is the same as fig. 2 of ref. [15]).

in the unfavored states larger when the core bears the O(6) character [16]). As for the $\gamma(-)$ components, the tendency is the same as our quasiparticle-vibration-coupling wave function as well as that of the signature-dependent effect on $B(\mathrm{E2}: I \to I-1)$ qualitatively*. On the other hand, the signature dependence of the mixing amplitudes of the $\gamma(+)$ components is opposite to our result, although the effect on the signature dependence of $B(\mathrm{E2}: I \to I-2)$ is similar. (See sect. 3 for the selection rule in our model.)

Before closing this section, we mention briefly the influence of static gamma deformation on properties of the quasiparticle-vibration-coupling wave function. We examined $\gamma^{(\rm pot)} = \pm 10°$ and $\pm 20°$. Resulting λ-dependence is similar to that in the $\gamma = 0$ case qualitatively but the structure shifts to the high-λ (low-λ) side when

* Unusually strong exchange interaction is necessary in order to make $B(\mathrm{E2}: \mathrm{f} \to \mathrm{u})$ larger than $B(\mathrm{E2}: \mathrm{u} \to \mathrm{f})$ in realistic calculations; ^{157}Ho case for example [17]).

negative (positive) gamma deformation is introduced. This is a consequence of the γ-dependence of ΔE in eq. (2.9); the zeros of the matrix elements of $Q_1^{(-)}$ and $Q_2^{(\pm)}$ shift depending on ΔE.* The effect on $B(\mathrm{E2}: I \to I-1)$ in $\gamma \neq 0$ cases will be discussed quantitatively in sect. 4.

3. Gamma-vibrational effects on B(E2)'s in axially symmetric nuclei

The effective principal-axis (PA) frame operators, which act on quasiparticle-vibration-coupling wave functions, for E2 ($\Delta I = 1, 2$) transitions are given by

$$\frac{1}{i} Q'^{(\mathrm{PA})}_{-1} = \sqrt{\frac{1}{2}}\left\{ -\sqrt{3}\langle Q_0^{(+)}\rangle \frac{J_z^{(\mathrm{qp})}}{I_0} + \langle Q_2^{(+)}\rangle \left(2\frac{iJ_y^{(\mathrm{qp})}}{I_0} + \frac{J_z^{(\mathrm{qp})}}{I_0} \right) \right\} + \frac{1}{i} Q'^{(\mathrm{vib})}_{-1} + \frac{1}{i} Q'^{(\mathrm{qp})}_{-1} ,$$

$$Q'^{(\mathrm{PA})}_{-2} = \langle Q'_{-2}\rangle + Q'^{(\mathrm{vib})}_{-2} + Q'^{(\mathrm{qp})}_{-2} , \tag{3.1}$$

where the operators Q'_μ ($\mu = -1, -2$) are quantized along the x-axis and are connected to $Q_K^{(\pm)}$ ($K = 0, 1, 2$) as

$$\frac{1}{i} Q'_{-1} = \sqrt{\tfrac{1}{2}}(Q_1^{(-)} - Q_2^{(-)}) ,$$

$$Q'_{-2} = \sqrt{\tfrac{1}{2}}(-\tfrac{1}{2}\sqrt{3} Q_0^{(+)} + Q_1^{(+)} - \tfrac{1}{2} Q_2^{(+)}) . \tag{3.2}$$

The vibrational terms are given by

$$\frac{1}{i} Q'^{(\mathrm{vib})}_{-1} = \sum_n \left\{ \left[X_{n(-)}, \frac{1}{i} Q'_{-1} \right]_{\mathrm{RPA}} X^\dagger_{n(-)} - \left[X^\dagger_{n(-)}, \frac{1}{i} Q'_{-1} \right]_{\mathrm{RPA}} X_{n(-)} \right\} ,$$

$$Q'^{(\mathrm{vib})}_{-2} = \sum_n \{ [X_{n(+)}, Q'_{-2}]_{\mathrm{RPA}} X^\dagger_{n(+)} - [X^\dagger_{n(+)}, Q'_{-2}]_{\mathrm{RPA}} X_{n(-)} \} . \tag{3.3}$$

The gamma-vibrational contributions to E2 matrix elements, picked up by these terms, appear in the first order with respect to the quasiparticle–vibration coupling. This fact makes discussion transparent in comparison with the case of routhians and M1 matrix elements**. The E2 ($\Delta I = 1$) matrix elements between the signature partners are given by [9])

$$\left.\begin{aligned} (\mathrm{f} \to \mathrm{u}) &\equiv \langle\langle \mathrm{u} | \frac{1}{i} Q'^{(\mathrm{PA})}_{-1} | \mathrm{f} \rangle\rangle \\ (\mathrm{u} \to \mathrm{f}) &\equiv \langle\langle \mathrm{f} | \frac{1}{i} Q'^{(\mathrm{PA})}_{-1} | \mathrm{u} \rangle\rangle \end{aligned}\right\}$$

* The qualitative relation between ΔE and the sign of $\langle \mathrm{f}|Q_1^{(-)}|\mathrm{u}\rangle / \langle \mathrm{f}|J_z|\mathrm{u}\rangle$ is valid also in $\gamma \neq 0$ cases although eq. (2.9) is not exact in such cases.

** The first-order contributions also exist in M1 matrix elements. But they are smaller than the second-order ones because of the difference in the multipolarity.

$$\simeq \sqrt{\frac{1}{2}}\Bigg\{ -\sqrt{3}\langle Q_0^{(+)}\rangle \frac{\langle \mathrm{f}|J_z|\mathrm{u}\rangle}{I_0} + \langle Q_2^{(+)}\rangle \Bigg(\mp 2 \frac{\langle \mathrm{f}|iJ_y|\mathrm{u}\rangle}{I_0} + \frac{\langle \mathrm{f}|J_z|\mathrm{u}\rangle}{I_0} \Bigg)$$

$$+ \frac{2}{\hbar\omega_{\gamma(-)}} (\chi_1^{(-)} (T_1^{(-)})^2 \langle \mathrm{f}|Q_1^{(-)}|\mathrm{u}\rangle \pm \chi_2^{(-)} (T_2^{(-)})^2 \langle \mathrm{f}|Q_2^{(-)}|\mathrm{u}\rangle)$$

$$+ (\langle \mathrm{f}|Q_1^{(-)}|\mathrm{u}\rangle \pm \langle \mathrm{f}|Q_2^{(-)}|\mathrm{u}\rangle) \Bigg\}, \tag{3.4}$$

where

$$\chi_1^{(-)} = \left(\frac{\omega_z' \omega_x'}{\omega_0^2}\right)^2 \kappa_1^{(-)}, \qquad \chi_2^{(-)} = \left(\frac{\omega_x' \omega_y'}{\omega_0^2}\right)^2 \kappa_2^{(-)}, \tag{3.5}$$

with

$$\omega_i' = \sqrt{\omega_i^2 - (1-\delta_{ix})\omega_{\mathrm{rot}}^2} \qquad (i = x, y, z),$$

$$\omega_0 = 41 A^{-1/3}\ \mathrm{MeV}/\hbar, \tag{3.6}$$

and I_0 being the angular momentum of the even-even core. The plus-minus sign in front of $\chi_2^{(-)}$ in eq. (3.4) has two consequences: first, it indicates that the (f→u) matrix element is larger (smaller) than the (u→f) at high (low) λ because the sign of $\langle \mathrm{f}|Q_2^{(-)}|\mathrm{u}\rangle$ is the opposite of (same as) that of $\langle \mathrm{f}|J_z|\mathrm{u}\rangle$ as shown in the top panel of fig. 1. Secondly, since $\langle \mathrm{f}|Q_1^{(-)}|\mathrm{u}\rangle$ and $\langle \mathrm{f}|Q_2^{(-)}|\mathrm{u}\rangle$ have the same sign in most cases [8,9]) (see the top panel of fig. 1), the $K=1$ and 2 components contribute constructively in the (f→u) while destructively in the (u→f).

The signature dependence of E2 ($\Delta I = 2$) matrix elements due to the $\gamma(+)$ vibration can be understood in a similar way. The first-order expression is given by

$$\langle\langle \mathrm{r}|Q_{-2}'^{(\mathrm{PA})}|\mathrm{r}\rangle\rangle = -\tfrac{1}{2}\sqrt{\tfrac{1}{2}}\{(\sqrt{3}\langle Q_0^{(+)}\rangle + \langle Q_2^{(+)}\rangle) + 2\delta_{\mathrm{r}}^{(+)}(\sqrt{3}\, T_0^{(+)} + T_2^{(+)})$$

$$+ (\sqrt{3}\langle \mathrm{r}|Q_0^{(+)}|\mathrm{r}\rangle + \langle \mathrm{r}|Q_2^{(+)}|\mathrm{r}\rangle)\}, \tag{3.7}$$

where r = f or u. Assuming $|\tilde{T}_2^{(+)}| \gg |\tilde{T}_0^{(+)}|$ (and $(T_2^{(+)}| \gg |T_0^{(+)}|$ at the same time) and $\omega_x' \simeq \omega_y'$, the vibrational term can be approximated by

$$\frac{2}{\hbar\omega_{\gamma(+)}} \chi_2^{(+)} (T_2^{(+)})^2 \langle \mathrm{r}|Q_2^{(+)}|\mathrm{r}\rangle, \tag{3.8}$$

with

$$\chi_2^{(+)} = \left(\frac{\omega_x'^2 + \omega_y'^2}{2\omega_0^2}\right)^2 \kappa_2^{(+)}. \tag{3.9}$$

Therefore, the signature dependence of $B(\mathrm{E2}: I \to I-2)$ due to the $\gamma(+)$ vibration is determined mainly by the deference between $\langle \mathrm{u}|Q_2^{(+)}|\mathrm{u}\rangle$ and $\langle \mathrm{f}|Q_2^{(+)}|\mathrm{f}\rangle$, as it is the case for the wave function (see fig. 1). Moreover, we can see from the expression (3.8) that the $\gamma(+)$ vibration enhances (reduces) the $B(\mathrm{E2})$ when $\langle \mathrm{r}|Q_2^{(+)}|\mathrm{r}\rangle$ is positive (negative) since the first term in the braces in eq. (3.7) is positive around $\gamma = 0$.

In both the $\Delta I = 1$ and 2 matrix elements, the vibrational terms contribute with the same sign as the corresponding odd-quasiparticle terms. This is consistent with the concept of the polarization charge, associated with gamma vibrations in the present case. We should note here that $e_{\rm pol}^{K(\pm)} \equiv 2\chi_K^{(\pm)}(T_K^{(\pm)})^2/\hbar\omega_{\gamma(\pm)}$ depends on K and $r = \pm 1$. The calculated values of $e_{\rm pol}^{2(\pm)}$ at $\hbar\omega_{\rm rot} = 0.2$ MeV are 14–21 whereas those of $e_{\rm pol}^{1(-)}$ stemming from the rotational K-mixing in the $\gamma(-)$ vibration are around 2. In ref. [6]), $e_{\rm eff}$ $(= e_{\rm pol} + 1) = 0.28 Q_0/\langle j|r^2|j\rangle$ was used as an input parameter. Assuming $Q_0/\langle j|r^2|j\rangle \sim O(Z)$, this value agrees with our calculated ones.

The signature dependence of B(E2)'s calculated under the same condition as fig. 1 is shown as a function of Z in the upper panel of fig. 2. This is a result of the diagonalization. In the expression (3.1), $I_0 = I - i_x$ and $I = \frac{17}{2}$ were assumed and i_x was calculated at the initial state of each nucleus. Their Z-dependence can be understood from the behavior of the single-quasiparticle quadrupole matrix elements shown in fig. 1. Note here that the weak signature dependence of the cranking value stems from the odd-quasiparticle terms. In the lower panel, they are presented as ratios to the corresponding cranking values without vibrational contributions. The shell-filling dependence predicted in the analytic study above is realized qualitatively but the ratios are compressed due to the increase in the norm of wave functions.

Fig. 2 indicates that the gamma-vibrational effect on $B(\mathrm{E2}: I \to I-2)$ is weaker than that on $B(\mathrm{E2}: I \to I-1)$. See the scales of the ordinates. This is because the zeroth-order term proportional to $\langle Q_0^{(+)} \rangle$ is more dominant in the former than in the latter, in which this term is attenuated by the factor $\langle \mathrm{f}|J_z|\mathrm{u}\rangle / I_0$. In the next

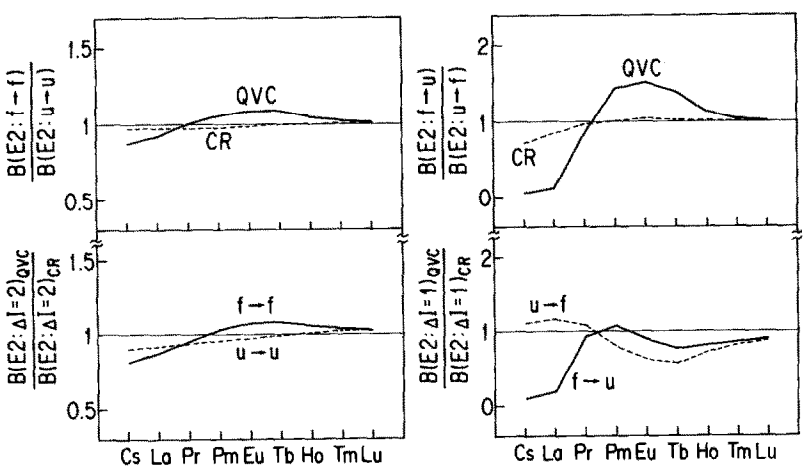

Fig. 2. Calculated ratios of $B(\mathrm{E2}: I \to I-2)$ (left) and $B(\mathrm{E2}: I \to I-1)$ (right). Note that the scale is different in the left and right. The signature dependence is shown in the upper panel while the magnitude of the vibrational contribution is shown in the lower panel. In $B(\mathrm{E2}: I \to I-1)$, $I_0 = I - i_x$ and $I = \frac{17}{2}$ were assumed (see eq. (3.1)). Other parameters are the same as in fig. 1. The values indicated by the solid line in the upper right figure are the same as fig. 3 of paper (I).

section, we will investigate the competition between the effects of static and dynamic triaxial deformations on $B(\mathrm{E2}: I \to I-1)$ based on the discussion in the present section.

4. Coherent effects of static and dynamic triaxialities on $B(\mathrm{E2}: I \to I-1)$

The vibrational effects on $B(\mathrm{E2}: I \to I-1)$ in axially symmetric nuclei have been discussed in the preceding section. In addition, static triaxial deformation also influences the transition rate. Here we should pay attention to the model dependence of its contents. In the cranking model, a triaxially deformed potential rotates around a principal axis and then its main effect on E2 ($\Delta I = 1$) matrix elements appears via $\langle Q_2^{(+)} \rangle$ in eq. (3.4). Consequently the signature dependence due to it depends on the sign of $\langle Q_2^{(+)} \rangle$ (see the dashed lines in fig. 2 of ref. [7])). On the other hand, static triaxial deformation in the particle-rotor model is accompanied by the fluctuation of the rotational axis. This is the reason why the signature dependence of $B(\mathrm{E2}: I \to I-1)$ in $\gamma = -15°$ case of ^{157}Ho in the particle-rotor calculation (the lower part of fig. 8 of ref. [18])) is inverted relative to the cranking result. As discussed in sect. 2 for the wave function, at least a part of the effect of the fluctuation can be taken into account by the quasiparticle-vibration coupling in our approach. Indeed, the gamma-vibrational contribution has inverted the signature dependence of the corresponding cranking result (see the solid lines in fig. 2 of ref. [7])).

This result indicates that the effect of the fluctuation is more important in the one-quasiparticle band of ^{157}Ho ($\Omega = \frac{7}{2}$) than that of the static deformation. In contrast, as shown in the upper part of fig. 8 of ref. [18]), the signature dependence is determined by the sign of $\langle Q_2^{(+)} \rangle \propto \sin\gamma$ also in the particle-rotor calculation when Ω/I is small. This ratio, Ω/I, is semiclassically related to the angle between the direction of the total spin and the cranking axis. The quasiparticle-vibration coupling treats the quantum fluctuation of this angle while the geometrical factor [19]) represents a permanent deviation of this angle from zero as a c-number. In the following, by making use of such a merit of the quasiparticle-vibration-coupling approach based on the cranking model that we can separate the effect of the static triaxial deformation of rotating potential itself and that of the fluctuation, we discuss the competition between them at a typical intermediate ω_{rot} treating γ as an input parameter. The geometrical factor is included in fig. 3 but it has nothing to do with the ratios in the other figures (see appendix of ref. [20])).

Numerical calculation was performed for $\gamma^{(\mathrm{pot})} = \pm 10°$ and $\pm 20°$ under the same condition as the $\gamma^{(\mathrm{pot})} = 0$ case which has been discussed already. The absolute magnitude of $B(\mathrm{E2}: I \to I-1)$ is shown in fig. 3 as a function of Z, both for the cranking and for the quasiparticle-vibration-coupling calculations. The λ-dependence of the signature-average value stems from that of $\langle \mathrm{f}|J_z|\mathrm{u} \rangle$ and $\langle Q_0^{(+)} \rangle$ in eq. (3.4) (see table 1). Their $\gamma^{(\mathrm{pot})}$ dependence can also be understood from expression (3.4).

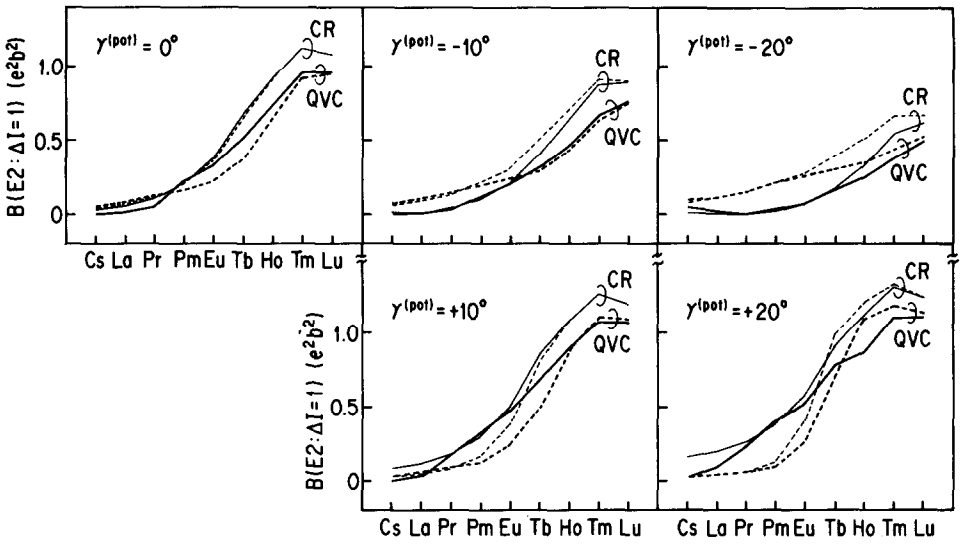

Fig. 3. $B(\mathrm{E2}: I \to I-1)$ calculated at each $\gamma^{(\mathrm{pot})}$. Solid and broken lines indicate the (f→u) and (u→f) transitions, respectively, both for the cranking and for the quasiparticle-vibration-coupling values. The sign of $\gamma^{(\mathrm{pot})}$ conforms to the Lund convention. The chemical potentials and the force strengths were determined in the same way as in the $\gamma = 0$ case (see the caption of fig. 1), but their values are slightly γ-dependent in general. The other parameters are the same as in fig. 2. In the geometrical factor, $\{1-(K/I)^2\}$ [ref. [20])], $K = \frac{1}{2}$ for Cs and La, $\frac{3}{2}$ for Pr and Pm, $\frac{5}{2}$ for Eu and Tb, $\frac{7}{2}$ for Ho and Tm, and $\frac{9}{2}$ for Lu were assumed.

In the cranking calculation, the signature dependence is determined uniquely by the sign of γ if the phase relation between $\langle \mathrm{f}|J_z|\mathrm{u}\rangle$ and $\langle \mathrm{f}|iJ_y|\mathrm{u}\rangle$ is normal. But for cases where $\gamma^{(\mathrm{pot})} > 0$, this relation, which is related closely to the signature inversion in quasiparticle energy and $B(\mathrm{M1})$ [ref. [15])], breaks down and consequently the signature dependence of $B(\mathrm{E2}: I \to I-1)$ is also inverted at the high λ. Fig. 4 shows that the vibrational effect itself magnifies the signature inversion in $B(\mathrm{E2}: I \to I-1)$ at the high-λ region in the positive-gamma cases. Except this point and the anomaly at the lowest λ due to the smallness of the cranking values in the negative-gamma cases, the global behavior of the gamma-vibrational contributions is almost independent of $\gamma^{(\mathrm{pot})}$ in the present calculation, in which the force strengths were chosen so as to reproduce $\hbar\omega_{\gamma(\pm)} = 0.8$ MeV at $\hbar\omega_{\mathrm{rot}} = 0$ irrespective of $\gamma^{(\mathrm{pot})}$.

The competition between the effects of static and dynamic triaxialities can be seen in fig. 5, which is the extension of the conclusion of paper (I) to $\gamma \neq 0$ cases. For $|\gamma^{(\mathrm{pot})}| = 10°$, the signature dependence due to gamma vibration:

$$B(\mathrm{E2}: \mathrm{f} \to \mathrm{u}) \gtrless B(\mathrm{E2}: \mathrm{u} \to \mathrm{f}) \qquad \text{for } \lambda \gtrless^{\exists} \lambda_{\mathrm{crit}} \tag{4.1}$$

survives except the weak signature inversion at Tm and Lu in the positive-gamma case. In contrast, the ratio is always smaller than unity for $\gamma^{(\mathrm{pot})} = -20°$ while it is

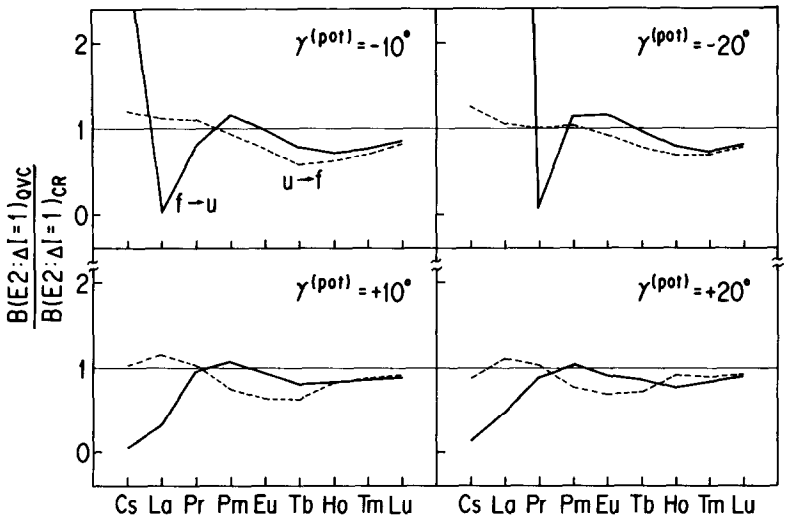

Fig. 4. Same as the lower right panel of fig. 2 but for $\gamma^{(pot)} = \pm 10°$ and $\pm 20°$. Parameters used are the same as in fig. 3.

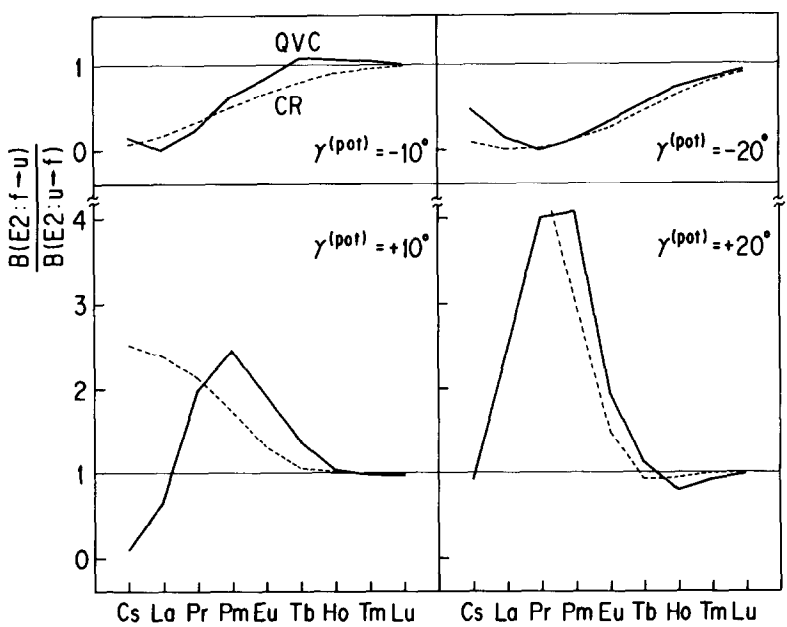

Fig. 5. Same as the upper right panel of fig. 2 but for $\gamma^{(pot)} = \pm 10°$ and $\pm 20°$. Parameters used are the same as in fig. 3.

larger than unity for $\gamma^{(\mathrm{pot})} = +20°$ except at the signature-inversion region and at Cs. In other words, the effect of static gamma deformation is stronger than that of gamma vibration at $|\gamma^{(\mathrm{pot})}| = 20°$. The zero-point amplitude γ_0 associated with gamma vibration calculated at $\hbar\omega_{\mathrm{rot}} = 0$ and $\gamma^{(\mathrm{pot})} = 0$ is tabulated in table 1. According to it, we can conclude that the selection rule (4.1) holds for the nuclei situated at the vibrational region, $|\gamma^{(\mathrm{pot})}| < \gamma_0$, whereas the signature dependence is determined by the sign of $\gamma^{(\mathrm{pot})}$ when $|\gamma^{(\mathrm{pot})}|$ is larger than γ_0.

Next we discuss the meaning of γ in the present approach. Three different standpoints are possible for how to take account of the shape polarization effect of the odd quasiparticle. The first is such that the polarization effect can be taken into account by the equilibrium shape of the even-even core and the coupling between the quasiparticle moving in the potential with this shape and the vibration of the core around this shape. This accords with the nuclear field theoretical approach. We have been based on this standpoint (see e.g. ref. [8])). Then, due to the collective rotation of the core, negative-gamma deformation is appropriate for one-quasiparticle bands. Therefore, the upper panel of fig. 5 is adequate for this case. For three-quasiparticle bands of $N = 90$ isotones, the equilibrium γ's of the s-bands are positive [21,8]). Therefore, the situation may correspond to the lower panel of fig. 5. But, since the calculated collectivity of $s\gamma$ phonons - gamma-vibrational phonons built on the s-band configuration - is weak [22,8]), the pattern of the broken line in this figure is expected to be realized.

The second standpoint is such that the shape polarization effect of the odd quasiparticle can be taken into account just by using the equilibrium shape of the odd-mass system, not that of the even-even core. In this case, the shape is in general signature dependent [see ref. [23]) for example]. A numerical example calculated by using the method based on the isotropic-velocity-distribution condition [21]) is shown in fig. 6. This result can be understood as a combined effect of collective rotation

TABLE 1

$B(\mathrm{E2}: 2_\gamma \to 0_g)$, $\langle Q_0^{(+)} \rangle$ and the zero-point amplitude γ_0 calculated at $\hbar\omega_{\mathrm{rot}} = 0$ and $\gamma^{(\mathrm{pot})} = 0$. Other parameters are the same as in fig. 1

Z	$B(\mathrm{E2}: 2_\gamma \to 0_g)$ (e^2b^2)	$\langle Q_0^{(+)} \rangle$ [a] (eb)	γ_0
$_{55}$Cs	0.02155	1.073	17.5°
$_{57}$La	0.02400	1.204	16.5°
$_{59}$Pr	0.02597	1.333	15.5°
$_{61}$Pm	0.02882	1.445	15.1°
$_{63}$Eu	0.03159	1.533	14.9°
$_{65}$Tb	0.03328	1.599	14.6°
$_{67}$Ho	0.03450	1.638	14.5°
$_{69}$Tm	0.03618	1.649	14.8°
$_{71}$Lu	0.03772	1.640	15.2°

[a]) The factor $\sqrt{5/16\pi}$ is included.

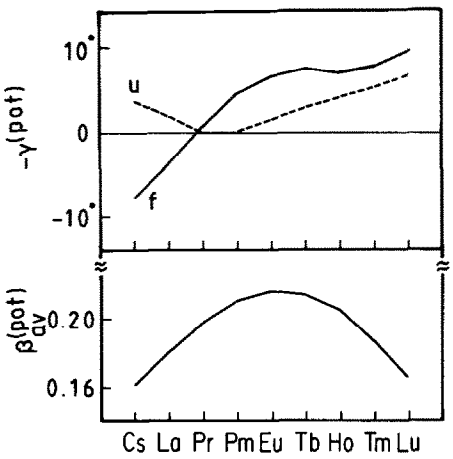

Fig. 6. Equilibrium deformations of the odd-A system calculated by means of the isotropic-velocity-distribution condition [21]) at $\hbar\omega_{rot} = 0.2$ MeV assuming $\Delta_n = \Delta_p = 1.0$ MeV. Since the signature dependence of the calculated β is weak, the signature-average value $\beta_{av}^{(pot)}$ is shown.

and the shape driving force of the odd quasiparticle determined by the matrix element of $Q_2^{(+)}$ (see the top left panel of fig. 1). It was shown in ref. [24]) that the calculated signature splitting of quasiparticle routhian was improved phenomenologically by inputting the signature-average γ of the odd-mass system to the even-even reference configuration in the cranking description. Assume this approach is valid also for transition rates, then

$$B(\mathrm{E2}:\mathrm{f}\to\mathrm{u}) \lesssim B(\mathrm{E2}:\mathrm{u}\to\mathrm{f}) \qquad \text{for } \lambda \gtrsim^{\exists} \lambda'_{crit} \tag{4.2}$$

holds qualitatively since the equilibrium γ_{av} is negative for the high λ and slightly positive for the low λ as shown in fig. 6. Note that λ'_{crit} does not necessarily coincide with λ_{crit} in eq. (4.1) in general. This selection rule may be realized in some cases in which the vibrational effect is weak and the equilibrium γ is determined predominantly by the odd quasiparticle: the three-quasiparticle bands of $N = 92$ isotones, where the aligned $(\nu i_{13/2})^2$ produces almost no γ-driving effect (see fig. 4 of ref. [21])), for example.

The third standpoint is such that both the shape driving force of the odd quasiparticle and the quasiparticle-vibration coupling should be taken into account. Comparing the selection rules (4.1) and (4.2), their effects are in the opposite direction of each other, although the origin of both mechanisms can be traced back to the shell-filling dependence of the quadrupole matrix elements shown in fig. 1.

The second approach seems insufficient because the fluctuation of the rotation axis is neglected there completely. At the present stage, it is an open question which is appropriate, the first or the third. This should be studied from the many-body theoretical viewpoint.

5. B(E2: $I \to I-1$) in Yb isotopes

The coherent effects of static and dynamic triaxialities have been studied in the preceding section for the $\pi h_{11/2}$ bands of $N=90$ isotone chain in detail. This chain was selected originally in order to explain the relation between the result of Onishi *et al.* [5]) and that of Ikeda [4]) and ours [7,8]) (see paper (I)). But, from the experimental point of view, it is difficult to reach the low-λ nuclei of this chain. Referring to this fact, we apply our model to an experimentally accessible case, the $\nu i_{13/2}$ bands of $^{159\text{-}169}$Yb. For $^{161\text{-}167}$Yb, $B(\mathrm{M1}: I \to I-1)/B(\mathrm{E2}: I \to I-2)$ was reported [25]), and E2/M1 mixing ratios are also known both for the (f→u)* and for the (u→f) transitions in ^{161}Yb and ^{169}Yb [the data were compiled in ref. [26])].

The calculation was performed at $\hbar\omega_{\mathrm{rot}}=0.2$ MeV under the same condition as in ref. [8]), where the equilibrium shapes of the core, the signature splitting of quasiparticle routhian and the B(M1) value were presented for ^{161,163,167}Yb. Additional parameters are $I=\frac{19}{2}$ and $i_x=3.0$ for $I_0=I-i_x$ in eq. (3.4). The signature dependence of B(E2: $I \to I-1$) is shown in fig. 7 in the same manner as in fig. 5. The calculated $\gamma^{(\mathrm{pot})}$ ranges from $-4.6°$ for ^{159}Yb to $-2.5°$ for ^{169}Yb. Since these values are smaller than the zero-point amplitude γ_0, a similar pattern to the $\pi h_{11/2}$ case with $\gamma^{(\mathrm{pot})}=0$ is realized.

The slope change of the solid line at $N=91$ in fig. 7 indicates the sign change of the matrix element of the (f→u) transition. This is measurable as the sign change of E2/M1 mixing ratio δ since the behavior of the M1 matrix element is known. Hagemann and Hamamoto pointed out recently the sign change of δ(u→f) due to M1 [ref. [26])]. In contrast, discussed at present is the sign change of δ(f→u) due to E2.

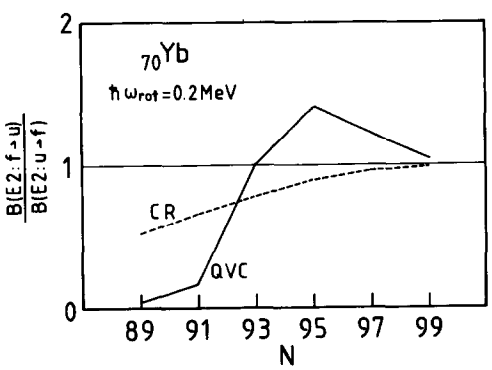

Fig. 7. Ratio of B(E2: $I \to I-1$) at $\hbar\omega_{\mathrm{rot}}=0.2$ MeV for Yb isotopes. The shape and pair deformations, β, γ, Δ_n and Δ_p were calculated selfconsistently adopting the isotopic-velocity-distribution condition [21]) and $G_n=2.64\,\hbar\omega_0/A$, $G_p=3.51\,\hbar\omega_0/A$. For ^{161,163,167}Yb, they were shown in figs. 12-14 of ref. [8]). $I_0=I-i_x$, $I=\frac{19}{2}$ and $i_x=3.0$ were assumed.

* Data were taken of the transition $(I-1)_u \to I_f$ instead of $I_f \to (I-1)_u$ in the low-λ nuclei in which the signature splitting is large.

The square of the mixing ratio is defined as

$$\delta^2 = \frac{T(\mathrm{E2}: I \to I-1)}{T(\mathrm{M1}: I \to I-1)}, \tag{5.1}$$

with $T(\lambda)$ being the transition probability with multipolarity λ. The reduced matrix element in the present model is given by

$$\langle I_\mathrm{f} \| T^{(\mathrm{L})}_\lambda \| I_\mathrm{i} \rangle = \sqrt{2I_\mathrm{i}+1}\langle I_\mathrm{i} I_\mathrm{i} \lambda I_\mathrm{f} - I_\mathrm{i} | I_\mathrm{f} I_\mathrm{f} \rangle \langle \chi_\mathrm{f} | T^{(\mathrm{PA})}_{\lambda, I_\mathrm{f}-I_\mathrm{i}} | \chi_\mathrm{i} \rangle , \tag{5.2}$$

with $|\chi\rangle$'s denoting intrinsic quasipartile-vibration-coupling states, and the superscripts (L) and (PA) indicate the laboratory frame and principal-axis frame components, respectively. Referring to it, the sign of δ is chosen as

$$\delta(I \to I-1) = 8.35 \times 10^{-3} \sqrt{\frac{I-1}{I+1}} \frac{\langle \chi_\mathrm{f} | Q'^{(\mathrm{PA})}_{-1} | \chi_\mathrm{i} \rangle}{\langle \chi_\mathrm{f} | \mu^{(\mathrm{PA})}_{-1} | \chi_\mathrm{i} \rangle} E_\gamma , \tag{5.3}$$

with $\langle \chi_\mathrm{f} | Q'^{(\mathrm{PA})}_{-1} | \chi_\mathrm{i} \rangle$ in $e \cdot \mathrm{fm}^2$, $\langle \chi_\mathrm{f} | \mu^{(\mathrm{PA})}_{-1} | \chi_\mathrm{i} \rangle$ in μ_N and the transition energy E_γ in MeV. In actual calculations, δ / E_γ was calculated microscopically at $\hbar\omega_\mathrm{rot} = 0.2$ MeV with

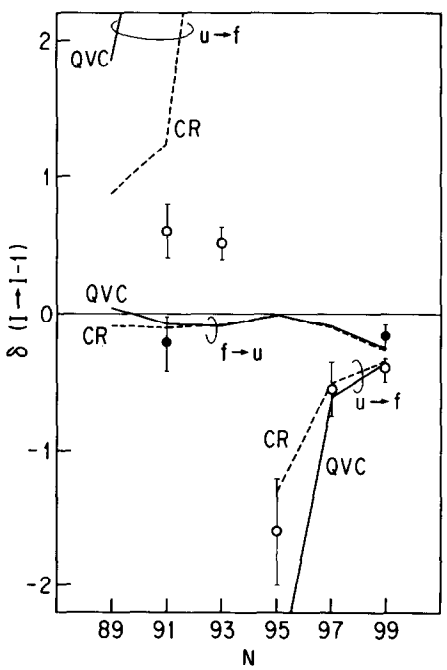

Fig. 8. E2/M1 mixing ratios of the (f→u) and (u→f) transitions. The latter diverges between $N = 93$ and $N = 95$ both in calculation and in experiment. Solid and broken lines indicate the calculated values with and without the coupling with gamma vibration, respectively. The M1 matrix elements were calculated assuming $g_\mathrm{R} = 0.2$. For ^{161,163,167}Yb, they were shown in figs. 19-21 of ref. [8]). For the E2 matrix elements, see fig. 7. In the calculated δ, E_γ's were taken from the data [25,27-30]). Experimental values of the (f→u) and (u→f) transitions are indicated by solid and open circles, respectively.

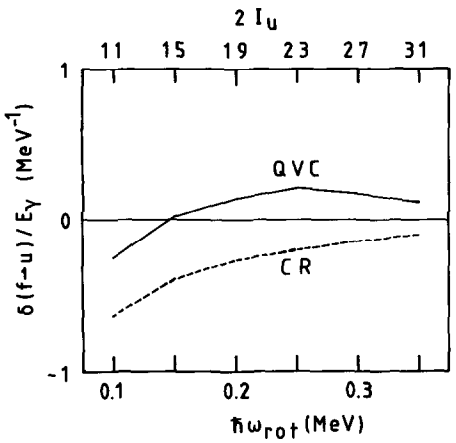

Fig. 9. The rotational-frequency dependence of $\delta(\mathrm{f}\rightarrow\mathrm{u})/E_\gamma$ calculated for ^{159}Yb. Assumed spin I is indicated for each ω_{rot}. At every ω_{rot}, $i_x = 3.0$ was assumed.

$I = \frac{19}{2}$ in the right-hand side, and E_γ's were taken from the data [ref. [27]) for ^{159}Yb, ref. [28]) for ^{161}Yb, ref. [25]) for ^{163}Yb, ref. [29]) for ^{165}Yb and ^{167}Yb, and ref. [30]) for ^{169}Yb]; $E_\gamma(\frac{19}{2}\rightarrow\frac{17}{2})$ for the (u→f) transitions and $E_\gamma(\frac{21}{2}\rightarrow\frac{19}{2})$ for the (f→u) transitions.

The numerical result is shown in fig. 8. This indicates that the calculation presented here (and therefore in ref. [8])) reproduces the sign change of the M1(u→f) matrix element between $N = 93$ and 95. At the higher-λ side, δ(u→f) is reproduced well. But, at the lower-λ side, the calculated values are larger than the experimental ones due to the smallness of the calculated M1 matrix elements (see figs. 19 and 20 of ref. [8])). As for δ(f→u), data are available only for ^{161}Yb and ^{169}Yb. Our calculation reproduces them well. The most important point is the sign change between $N = 89$ and 91 due to E2 although from an experimental point of view it seems difficult to measure this effect. This corresponds to the slope change in fig. 7 mentioned above. This is another consequence of the coupling with gamma vibration. The ω_{rot} dependence is shown in fig. 9. This illustrates that the vibrational contribution becomes important as the rotational contribution proportional to $1/I_0$ (see eq. (3.1)) becomes small if the collectivity of the phonon survives.

6. Concluding remarks

We have extended the study on the gamma-vibrational effect on $B(\mathrm{E2}: I\rightarrow I-1)$ by means of the quasiparticle-vibration-coupling approach based on the cranking model and RPA developed for the $\gamma = 0$ case in the preceding paper (paper (I)). The present paper consists of two parts. In the first half, properties of the quasiparticle-vibration-coupling wave function (in sect. 2) and of $B(\mathrm{E2}: I\rightarrow I-2)$ (in sect. 3) have been studied in a parallel manner with paper (I): their behavior has been

studied analytically in the first-order perturbation theory with respect to the quasiparticle-vibration-coupling hamiltonian and then numerical calculation has been performed in order to confirm the analytic results. The signature dependence and the shell-filling dependence of both quantities are determined by the properties of the single-quasiparticle matrix elements of quadrupole operator. In relation to the signature dependence of the wave function, the similarity and the difference between the coupling schemes in the present approach, the particle-rotor model and the interacting boson-fermion model have also been discussed. The gamma-vibrational effect on $B(\mathrm{E2}: I \to I-2)$ is weaker than that on $B(\mathrm{E2}: I \to I-1)$.

In the second half, the competition between the effects of static and dynamic triaxialities on $B(\mathrm{E2}: I \to I-1)$ has been studied numerically. In sect. 4, the study in paper (I) has been extended directly to $\gamma \neq 0$ cases. The effect of gamma vibration defeats that of static gamma deformation when $|\gamma^{(\mathrm{pot})}|$ is smaller than the zero-point amplitude. The meaning of γ in the present approach has also been discussed. We have performed more realistic calculation for an experimentally accessible isotope chain, $^{159\text{-}169}$Yb in sect. 5. The calculation predicts that the characteristic signature dependence and the shell-filling dependence due to gamma vibration similar to those shown in paper (I) survive clearly, since the equilibrium gamma deformation is small. The sign change of E2/M1 mixing ratio stemming from the vibrational contribution has also been predicted. Experimental data are desired to test our prediction.

Stimulating discussions with K. Matsuyanagi and Y.R. Shimizu at the early stage of the present work are acknowledged. The computer code for the cranking model and RPA was provided by Y.R. Shimizu. The author is indebted to Fellowships of the Japan Society for the Promotion of Science for Japanese Junior Scientists. This work was supported by the Grant-in-Aid for Scientific Research from the Ministry of Education, Science and Culture (No. 01790182).

References

1) G.B. Hagemann *et al.*, Nucl. Phys. **A424** (1984) 365
2) D.C. Radford *et al.*, contribution to Workshop on nuclear structure, Copenhagen, 1988
3) I. Hamamoto and B.R. Mottelson, Phys. Lett. **B132** (1983) 7
4) A. Ikeda, Nucl. Phys. **A439** (1985) 317
5) N. Onishi *et al.*, Nucl. Phys. **A452** (1986) 71
6) I. Hamamoto and Z. Xing, Phys. Scr. **33** (1986) 210
7) M. Matsuzaki, Y.R. Shimizu and K. Matsuyanagi, Prog. Theor. Phys. **77** (1987) 1302
8) M. Matsuzaki, Y.R. Shimizu and K. Matsuyanagi, Prog. Theor. Phys. **79** (1988) 836
9) M. Matsuzaki, Nucl. Phys. **A491** (1989) 433
10) A. Ikeda and T. Shimano, contribution to Workshop on nuclear structure in the era of new spectroscopy part B, Copenhagen, 1989
11) Y.R. Shimizu and K. Matsuyanagi, Prog. Theor. Phys. **70** (1983) 144
12) M. Matsuzaki, Nucl. Phys. **A509** (1990) 269
13) I. Hamamoto, Phys. Lett. **B193** (1987) 399
14) I.N. Mikhailov and D. Janssen, Phys. Lett. **B72** (1978) 303

15) M. Matsuzaki, Nucl. Phys. **A504** (1989) 456
16) N. Yoshida *et al.*, Nucl. Phys. **A503** (1989) 90
17) H. Sagawa, private communication (1990)
18) I. Hamamoto, Nucl. Phys. **A421** (1984) 109c
19) F. Dönau, Nucl. Phys. **A471** (1987) 469
20) M. Oshima *et al.*, Phys. Rev. **C40** (1989) 2084
21) Y.R. Shimizu and K. Matsuyanagi, Prog. Theor. Phys. **71** (1984) 960
22) Y.R. Shimizu and K. Matsuyanagi, Prog. Theor. Phys. **72** (1984) 799
23) S. Frauendorf and F.R. May, Phys. Lett. **B215** (1983) 245
24) S. Shastry *et al.*, Nucl. Phys. **A470** (1987) 253
25) J. Kownacki *et al.*, Nucl. Phys. **A394** (1983) 269
26) G.B. Hagemann and I. Hamamoto, Phys. Rev. **C40** (1989) 2862
27) M.A. Lee, Nucl. Data Sheets **53** (1988) 507
28) M.J.A. de Voigt, J. Dudek and Z. Szymański, Rev. Mod. Phys. **55** (1983) 949
29) N. Roy *et al.*, Nucl. Phys. **A382** (1982) 125
30) E. Selin, A. Hjorth and H. Ryde, Phys. Scr. **2** (1970) 181